Technical report; TR-191

KNMI

Description and verification of the Hirlam trajectory model

E.I.F. de Bruijn

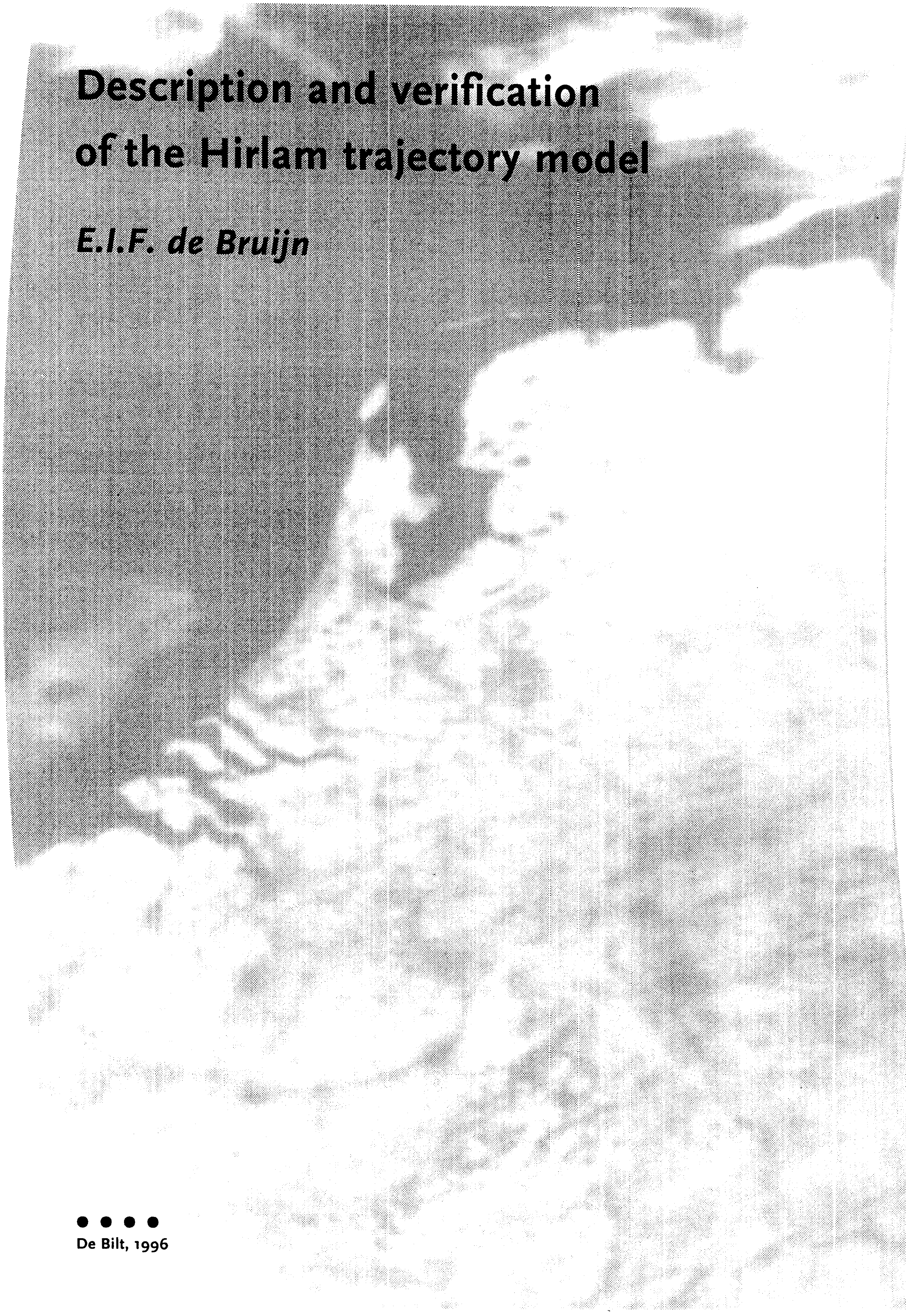

Koninklijk Nederlands Meteorologisch Instituut

De Bilt, 1996

Technical report; TR-191

De Bilt, 1996

Postbus 201
3730 AE De Bilt
Wilhelminalaan 10
Telefoon 030-220 69 11
telefax 030-221 04 07

Auteurs: E.I.F. de Bruijn

UDC: 551.509.313
551.509.51
551.511.6

ISSN: 0169-1708

ISBN: 90-369-2103-I

Description and verification of the HIRLAM trajectory model

E.I.F. de Bruijn

WM

February 1996

Contents

1 Introduction

Trajectories are used for several purposes at KNMI. Backward trajectories are used for finding the location where air comes from, the so-called source area. Going backwards from a receptor point with the use of the predicted windflow the upstream position of an airparcel can be determined. In the source area the airmass can be analysed by radiosonde observations. Additional cloud-cover information can be retrieved from satellite imaging. Transporting the airmass with its clouds along the trajectory gives the forecaster an idea of the predicted cloudiness and vertical structure of the atmosphere at the receptor point. At KNMI a trajectory model was developed and implemented at the European Centre in Reading. The source code of the model is redesigned and modified for computing trajectories on High Resolution Limited Area Model (HIRLAM) fields. The trajectory model can run both on predicted and on analyzed fields. Comparing the results leads to the demand for an objective verification system. In the literature such a method was found (Rolph et al. [3]); it was slightly modified for the calculation of distances and implemented at KNMI.

In this report HIRLAM, which is used for forecasting purposes, is described in more detail. The method for computing the vertical motion from the horizontal wind fields is described as well. Secondly the method of computation of HIRLAM trajectories is presented. Subsequently a method for verification of trajectories is described. Verification results for the months January and July 1995 are presented. A striking event with enormous differences between predicted and analyzed trajectories is finally presented as a case study.

Trajectories with a duration of 36 hours at 500 hPa level during January 1995 have horizontal and vertical deviations of about 600 km and nearly 100 hPa, respectively. Low level short trajectories of 12 hours at 975 hPa level during July 1995 have horizontal and vertical deviations of about 40 km and 5 hPa, respectively.

2 Description of HIRLAM

2.1 general aspects of HIRLAM

HIRLAM is a Numerical Weather Prediction Model (NWP) developed at the National Weather Services of Denmark, Finland, Iceland, Ireland, Sweden, Norway and the Netherlands. The actual HIRLAM work consists of: the preparation of the Analysis Observation File (AOF), the preparation of the boundary files which are extracted from ECMWF-forecasts, running the main modules of analysis, initialisation and forecast, and finally postprocessing. All HIRLAM products are archived in GRIB format with full horizontal and vertical resolution.

The integration area of the HIRLAM being operated at KNMI covers Europe and the North Atlantic and is a transformed latitude/longitude grid with the Southpole moved along the 0 meridian to the latitude of 30 S to avoid strong convergence of longitudes towards the pole. The integration domain consists of 92 $\times$ 81 gridpoints and 16 vertical levels. The horizontal gridpoint distance is 0.5 degrees which corresponds with 55 km. Four 36-hours forecasts are run daily with a timestep size of 5 minutes. The boundaries from ECMWF are based on the 1200 UTC run of the previous day. The boundaries are updated with the most recent of ECMWF 0000 UTC and 1200 UTC forecasts. The basic formulation of the HIRLAM model is the primitive equations with the hydrostatic assumption [4]. The prognostic variables are the horizontal velocity components, temperature, surface pressure and specific humidity. In addition a passive scalar is advected in three spatial dimensions by the semi implicit leapfrog method. The passive scalar is intended for the inclusion of cloud liquid water or alternatively some tracer of pollution. The physical parametrisation consists of large scale condensation, cumulus convection, vertical diffusion, radiation and surface processes.

2.2 vertical velocity

The vertical coordinate is the terrain following hybrid coordinate with sigma levels at the surface and pressure levels at the top. The definition of the orography is derived from US Navy data. The vertical velocity is calculated during the postprocessing and is based on the integration of the continuity equation in the vertical. It consists of two components

$$\omega = \omega_h + \omega_f \quad (1)$$

$$\omega_h = -\int_0^\eta \nabla \cdot (V\frac{\partial p}{\partial \eta})d\eta \quad (2)$$

$$\omega_f = V_{hor} \cdot \nabla p \quad (3)$$

ω_f is a correction factor for displacements in mountainous terrain and ω_h follows from the integration of the divergence of the horizontal wind in a layer up to the η level. The abovementioned method for calculating the vertical motion describes the large scale vertical motion and does not account for updrafts and downdrafts in convective cells.

3 Method of computation for trajectories

3.1 Displacement

Archived fields of the three windcomponents (u,v,w), the pressure at a model level p_i and the surface pressure p_s are required for the trajectory computations. The horizontal advection of a particle from an initial position (0) to a position (1) is defined as

$$\vec{H_1} = \vec{H_0} + \vec{v_0}\Delta t \quad (4)$$

where Δt is the time step, $\vec{H_0}$ and $\vec{H_1}$ are the horizontal position vectors at initial and first position respectively. $\vec{v_0}$ is the horizontal wind vector at the initial position $\vec{H_0}$. The next position is calculated according to

$$\vec{H_2} = \vec{H_0} + \frac{(\vec{v_o} + \vec{v_1})}{2}\Delta t \quad (5)$$

The wind vectors at the initial and first position are averaged. With the new windspeed the displacement is again calculated. To compute the vertical transport the pressure of the final position (2) is calculated with

$$p_2 = p_0 + \omega\Delta t \quad (6)$$

where ω is the average vertical velocity, $\frac{dp}{dt}$, between the initial position (0) and final position (2). This procedure is repeated until the differences between two consecutive values of $\vec{H}$ and p are less than $0.1\Delta x$ and 10 Pa, respectively. Δx is the mesh size of 55 km. This is the predictor-corrector method (Pettersen [2]) of computing trajectories which accounts for most of the curvature in the wind field. During the transport the airparcel can not penetrate into the soil. Near the surface the hybrid coordinate is like a σ coordinate, so the airparcel is terrain following and remains on the lowest model level.

3.2 Spatial interpolation

An air parcel will be seldom at the exact position of a grid point at a certain model level. Therefore interpolation of wind data to the position of the air parcel is required. In the horizontal plane a bilinear interpolation is used. The coordinates are given in degrees. If we choose a position (x,y) in a square G with coordinates (0,0),(1,0),(0,1),(1,1) the value relative to corner (0,0) can be calculated according

$$G_{x,y} = (1-x)(1-y) \cdot G_{0,0} + x(1-y) \cdot G_{1,0} + y(1-x) \cdot G_{0,1} + xy \cdot G_{1,1} \quad (7)$$

In the vertical plane the position relative to the surface is determined by

$$p_i = a_i + b_i \cdot p_s \quad (8)$$

p_i is the pressure at model level i, a_i,b_i are the coefficients which determine the hybrid coordinate system and p_s is the surface pressure. The values of a_i,b_i can be found in the appendix. With an iterative procedure the level above and below the actual position are calculated. Subsequently a linear interpolation is applied to obtain the interpolated windcomponents on the actual height of the air parcel.

$$\vec{v}(p_i) = \vec{v}(p_k) + \frac{(p_i - p_k)}{(p_l - p_k)}\vec{v}(p_l) \quad (9)$$

$\vec{v}(p_i)$ is the interpolated value of the wind vector at the actual pressure of the parcel. $\vec{v}(p_k)$ and $\vec{v}(p_l)$ are the windvectors at the model levels. p_i is the actual pressure of the parcel and p_l, p_k are the pressures of the model levels below and above, respectively.

3.3 Time interpolation

The time step Δt, see formula 4 can be freely choosen. If Δt is smaller than the temporal resolution of the predicted windfields an interpolation has to be carried out. The interpolated value can be obtained by a linear interpolation with two fields, corresponding with the two surrounding times. If we choose t for the actual time and t_1 en t_2 the times of the surrounding fields the interpolated value is obtained by

$$H(t) = H(t_1) + \frac{(t - t_1)}{(t_2 - t_1)} H(t_2) \tag{10}$$

where H represents the interpolated fields of wind speed and surface pressure.

3.4 Motion over the sphere

The displacement is calculated along a great circle from the initial position λ_i,φ_i to the final position λ_f,φ_f with the speed $\vec{u_i}$ and time step Δt. The initial and final position together with the northpole form a triangle on the (unit) sphere (Fig. 1).

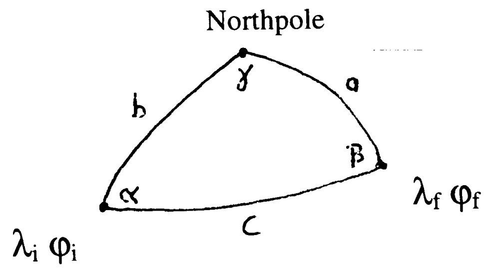

Figure 1: Triangle on the sphere with relevant distances and angles

The angles are defined as α,β,γ and the sides as a,b,c respectively. The sides correspond with distances over the sphere and they are expressed in radians. The following variables can be derived:

$$\alpha = arctan(\frac{u}{v}) \tag{11}$$

$$b = \frac{\pi}{2} - \varphi_i \tag{12}$$

$$c = \Delta t \cdot \frac{|\vec{u_i}|}{R} \tag{13}$$

R is the earth's radius. The factor $1/R$ transforms the actual velocity $|\vec{u_i}|$ to a velocity on the unit sphere. Applying the cosine rule and subsequently the sine rule yields

$$a = arccos(cos(b)\dot{c}os(c) + sin(b) \cdot sin(c) \cdot cos(\alpha)) \tag{14}$$

$$\gamma = arcsin(sin(c) \cdot \frac{sin(\alpha)}{sin(a)}) \tag{15}$$

The final position (λ_f,φ_f) is calculated according $\varphi_f = \frac{\pi}{2} - a$ and $\lambda_f = \lambda_i + \gamma$

3.5 Averaging of the windspeed

In order to calculate the displacements properly the windspeeds at the initial and end position have to be averaged (see formula 5). The windspeed is based on the local north vector. In the chosen coordinate system the local north vector is dependent of its position. The wind speed in the initial and final position can not be simply averaged. Therefore the final speed $\vec{u}_f$ has to be transformed by a linear transformation to the coordinate system of the initial position

$$R_\theta = \begin{pmatrix} cos(\theta) & -sin(\theta) \\ sin(\theta) & cos(\theta) \end{pmatrix} \tag{16}$$

Applying $\vec{u}'_f = R_\theta \cdot \vec{u}_f$ gives the transformed wind speed. The rotation angle θ can be estimated as $\theta = (\lambda_f - \lambda_i) \cdot sin(\varphi_i)$

3.6 Objective verification of trajectories

The mean deviation between a set of forecasted trajectories and the corresponding true trajectories is determined by the mean absolute horizontal transport deviation AHTD. The trajectories based on analysed fields are considered as true trajectories

$$AHTD(t) = \frac{1}{N} \sum_{n=1}^{N} d(\lambda_t^n, \lambda_f^n, \varphi_f^n, \varphi_t^n) \tag{17}$$

t corresponds with the travel time and varies between 0 and 36 hours with a step size of three hours. N is the number of trajectories and equals the product of the number of trajectory levels and the number of arrival stations. d is the distance between two positions (λ_f,φ_f) and (λ_t,φ_t) on the sphere:

$$d = R \cdot arccos(cos(\lambda_t - \lambda_f) \cdot cos(\varphi_t) \cdot cos(\varphi_f) + sin(\varphi_t) \cdot sin(\varphi_f)) \quad (18)$$

where R denotes the earth radius. (λ_t,φ_t) and (λ_f,φ_f) are the geographical coordinates for the true and forecasted trajectory respectively. The mean absolute vertical transport deviation AVTD is given by

$$AVTD(t) = \frac{1}{N} \sum_{n=1}^{N} |p_f^n - p_t^n| \quad (19)$$

where p_f and p_t represent the vertical coordinate of the forecasted and true trajectory respectively.

Another useful statistical concept is the mean relative horizontal transport deviation RHTD. This is defined as the ratio between the absolute transport deviation and the mean total travel distance of the true trajectories

$$RHTD(t) = \frac{AHTD(t)}{L_H(t)} \quad (20)$$

where $L_H(t)$, the mean absolute horizontal travel distance of the true trajectories is defined as

$$L_H(t) = \frac{1}{N} \sum_{n=1}^{N} \sum_{i=1}^{t} d(\lambda_t^n, \lambda_{t-1}^n, \varphi_t^n, \varphi_{t-1}^n) \quad (21)$$

d is the abovementioned function (18). Similarly, the mean relative vertical transport deviation RVTD is

$$RVTD(t) = \frac{AVTD(t)}{L_v(t)} \quad (22)$$

where $L_v(t)$, the mean absolute vertical travel distance of the true trajectories is defined as

$$L_v(t) = \frac{1}{N} \sum_{n=1}^{N} \sum_{i=1}^{t} |p_t^n(t) - p_t^n(t-1)| \quad (23)$$

Here $\lambda_t^n(t)$,$\varphi_t^n(t)$ and $p_t^n(t)$ are the coordinates of a true trajectory at time t, and $\lambda_t^n(t-1)$,$\varphi_t^n(t-1)$ and $p_t^n(t-1)$ are the parcel coordinates at the previous time. The positions are summed for times between 1 and t

4 Verification of HIRLAM trajectories

4.1 General setup

Predicted and analyzed fields of HIRLAM are currently available in the archives. The spatial and temporal resolution of the meteorological data are 55 km and 3 hours, respectively. To obtain a good quality trajectory the time step must be chosen in such a way that the trajectory program still gives reliable results even when rapidly moving synoptic systems pass. The computations are performed with a timestep Δt of thirty minutes (see eq. 4). The months January and July of 1995 are selected for the verification of the backward trajectories. Every day two series are calculated at 0000 and 1200 UTC. The series consist of trajectories with a forecast period of 12,24 and 36 hours for six locations covering the area of Holland. It should be noted that the trajectories arrive at different times. The locations are K13, De Kooy, Eelde, De Bilt, Vlissingen and Beek. The trajectories are verified on the 975 and 500 hPa level which are typical for the boundary layer and the free atmosphere, respectively. The calculated absolute and relative deviations are monthly averages of January and July in 1995. The standard deviation is calculated according $\sigma_x = \sqrt{\frac{(x-\overline{x})^2}{n-1}}$ where x denotes AHTD(t),AVTD(t), RHTD(t), RVTD(t) and n is the number of forecast series per month during January and July in 1995. When the trajectories leave the horizontal domain they are terminated. Trajectories that intercept the model surface stay at the lowest sigma level until their vertical velocity changes direction. Unfortunately 5 percent of trajectories could not be calculated due to discrepancies in the archive.

4.2 The most important results of the experiment

The most important results of the experiment are summarized in Tables 1 and 2 for average and relative deviation statistics and their standard deviations for 12, 24 and 36 hours of travel time and for levels of 975 and 500 hPa.

	975 hPa				500 hPa			
t	AHTD	σ_{AHTD}	RHTD	σ_{RHTD}	AHTD	σ_{AHTD}	RHTD	σ_{RHTD}
-12	89 km	60 km	3.1	1.8	101 km	56 km	1.9	1.6
-24	221 km	129 km	3.9	2.4	361 km	224 km	3.5	3.4
-36	418 km	317 km	5.0	4.6	580 km	419 km	3.7	2.6
	AVTD	σ_{AVTD}	RVTD	σ_{RVTD}	AVTD	σ_{AVTD}	RVTD	σ_{RVTD}
-12	20 hPa	12 hPa	10.9	7.7	32 hPa	21 hPa	7.7	4.1
-24	38 hPa	24 hPa	8.7	6.0	85 hPa	54 hPa	9.9	5.8
-36	53 hPa	30 hPa	7.6	4.8	111hPa	58 hPa	10.4	5.1

Table 1: Average and relative deviation statistics during January 1995. The relative deviation statistics are given in percents

	975 hPa				500 hPa			
t	AHTD	σ_{AHTD}	RHTD	σ_{RHTD}	AHTD	σ_{AHTD}	RHTD	σ_{RHTD}
-12	37 km	22 km	2.7	2.0	50 km	35 km	2.0	1.6
-24	106 km	59 km	3.6	2.1	192 km	117 km	3.5	2.5
-36	212 km	161 km	4.1	2.7	377 km	271 km	4.0	2.5
	AVTD	σ_{AVTD}	RVTD	σ_{RVTD}	AVTD	σ_{AVTD}	RVTD	σ_{RVTD}
-12	6 hPa	3 hPa	6.3	2.8	16 hPa	9 hPa	8.7	4.6
-24	14 hPa	7 hPa	7.5	3.5	41 hPa	37 hPa	8.9	4.6
-36	24 hPa	11 hPa	8.0	3.8	54 hPa	51 hPa	9.3	4.6

Table 2: Average and relative deviation statistics during July 1995. The relative deviation statistics are given in percents

Both horizontal (AHTD) and vertical (AVTD) deviations and their repective σ values increase with travel time and with level of transport. The maximum value for the AHTD and AVTD are 580 km and 111 hPa, respectively for the 36 hours 500 hPa trajectory in January 1995. The corresponding σ_{AHTD} and σ_{AVTD} are 419 km and 58 hPa, respectively. This means that the distribution of the deviations is not sharply peaked around a mean value. The quality of the trajectories varies from day to day. Near the surface in the summer month July with relatively low windspeeds the horizontal and vertical deviations are 25 km and 6 hPa, respectively for the 12 hours 975 hPa trajectory. The relative horizontal deviations (RHTD) increases with the forecast time. The 975 and the 500 hPa trajectory have relative horizontal deviations between 2 and 4 percent. The relative vertical deviations (RVTD) vary between 6 and 11 percent.

4.3 Average statistics for 36 hours trajectories

Fig. 2 shows the complete AHTD statistics for the 36 hours trajectories during January and July 1995. Plotted on each graph are the results for the levels 975 and 500 hPa during the abovementioned months. It is clear from Fig. 2 that AHTD increases with travel time and level of transport. During July the deviations are smaller than in January. In January higher windspeeds occur frequently, resulting in trajectories which reach the borders of the horizontal domain. At the borders the trajectory stops which leads to inaccurate results and big deviations. In Fig. 2 at -12 hours the AHTD of the 500 hPa trajectory is 236 and 142 km for January and July 1995, respectively. In the tables 1 and 2 we see for the 12 hours trajectory at 500 hPa has an AHTD of 101 and 50 km, respectively. The difference can be explained by stating that the 12 hours trajectory is not a part of the 36 hours trajectory. Albeit they are based on the same analysis, they have different arrival times and thus different deviations.

4.4 Relative statistics for 36 hours trajectories

In Figs. 4 and 5 the complete RHTD and RVTD statistics of the 36 hours trajectories are presented. From Fig. 4 and 5 it is obvious that initially the RHTD and RVTD are rather high and they decrease with travel time. In the first three hours of travel time substantial differences between forecasted and

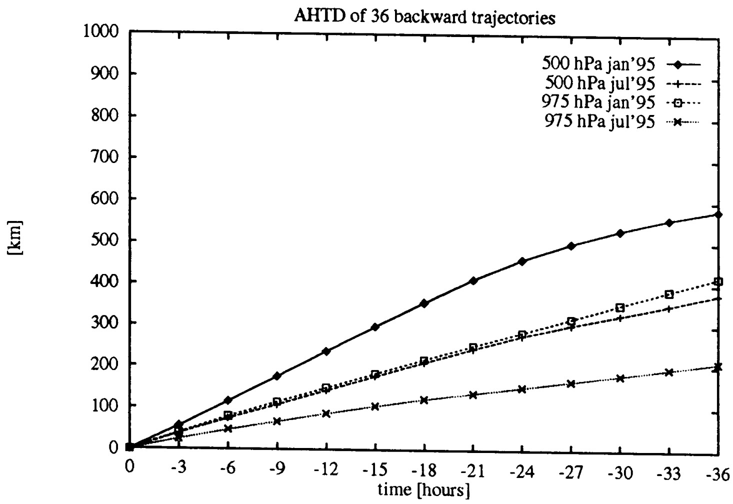

Figure 2: AHTD of 36 hours trajectories during January and July 1995

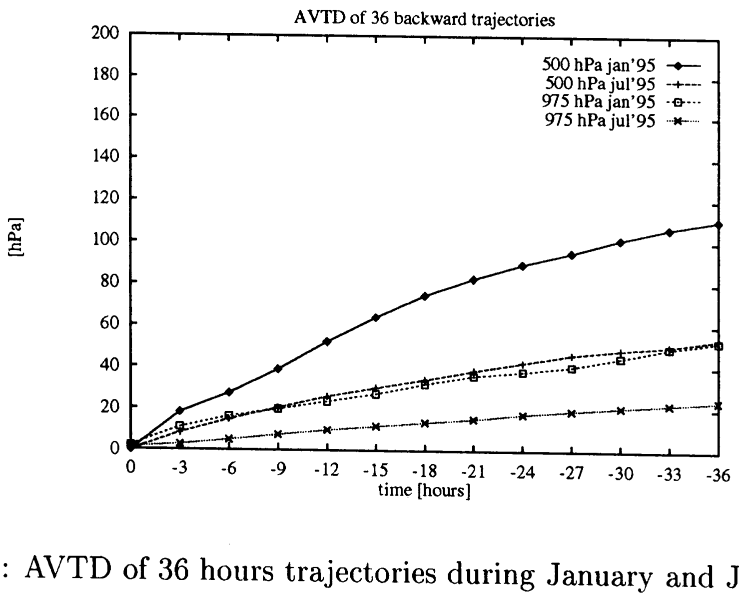

Figure 3: AVTD of 36 hours trajectories during January and July 1995

analysed windfields may occur due to initialisation errors. During this period any errors associated with differences between forecast and analysed fields are accumulated in the trajectory error. As travel time increases the forecast-initialization error is expected to remain constant and becomes overruled by the increasing trajectory errors. From Fig. 4 and 5 it is clear that the RVTD is larger than the RHTD. The initialization process which balances the wind fields and mass fields, results in a reduction of the divergence of the horizontal windfield. This has more impact on the vertical velocity than on the horizontal windfield. The vertical velocity is strongly related to the divergence (see eq. 3). At three hours back the RVTD starts with values around 25 percent. With increasing time they reduce to values of about 12 percent. The RHTD in Fig. 4 starts at three hours back at values between 4 and 8 percent. With increasing travel time the RHTD slightly decreases to values between 4 and 6 percent. The 975 hPa trajectory has a bigger RHTD value than the 500 trajectory. At higher levels with the longer travel distances the RHTD's are reduced. In summer time moderate winds prevail resulting in 36 hours trajectories who stay in the horizontal domain of the HIRLAM.

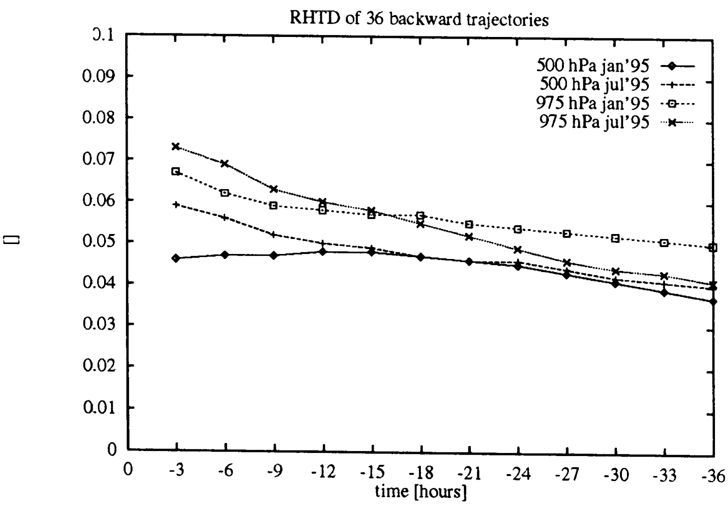

Figure 4: RHTD of 36 hours trajectories during January and July 1995

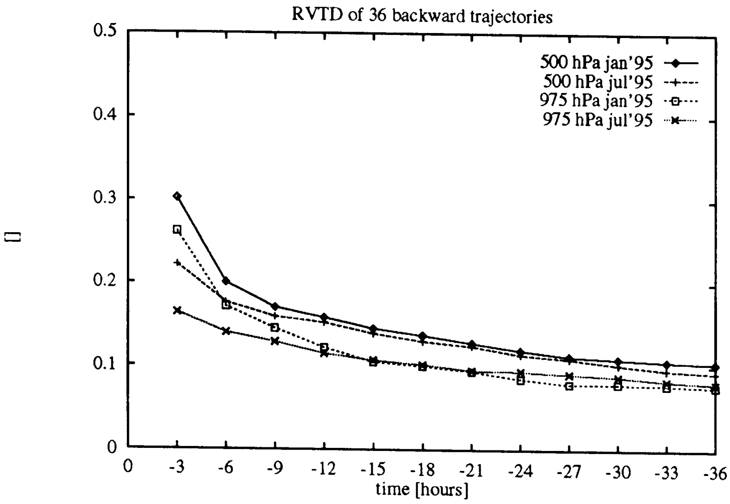

Figure 5: RVTD of 36 hours trajectories during January and July 1995

4.5 Case study of an extreme situation

The accuracy of the trajectory computation is affected by several sources of error. The Pettersen scheme [2] used in the computation has a second order accuracy. It accounts for most of the curvature in the wind field, except in those cases where large gradients in the wind field are present. The meteorological situation can thus lead to substantial uncertainty in the trajectory calculation. This effect will be aggravated by forecast errors from the model supplying the windfield. Even small errors in the forecast of the position of gradients in the wind field may amplify in the trajectory calculation. Similarly analysis errors will affect the calculation of 'true' trajectories. All these effects show up in the verification statistics presented in this report.

The divergence of trajectories starting from or arriving at nearby locations may give a good indication of the sensitivity of the trajectory calculation to model analysis and forecast errors and thus reveal a mesure of uncertainty, which ought to be reflected in verification statistics. This will be demonstrated in this case study.

From the dataset of 124 cases we have chosen 1 January 1995 for a more detailed evaluation, because the largest deviation occured in this case. In Fig. 6 the HIRLAM +1800 hours forecast of the geopotential height at 500 hPa is shown. The analysis time of this forecast series is 0000 UTC. A low pressure system is situated above South Sweden and moves slightly in north easterly direction. On the Atlantic Ocean a ridge is building up. For the Netherlands this results in a north westerly flow with advection of cold air over the relatively warm North Sea. In Fig. 7 and 8 the forecasted and

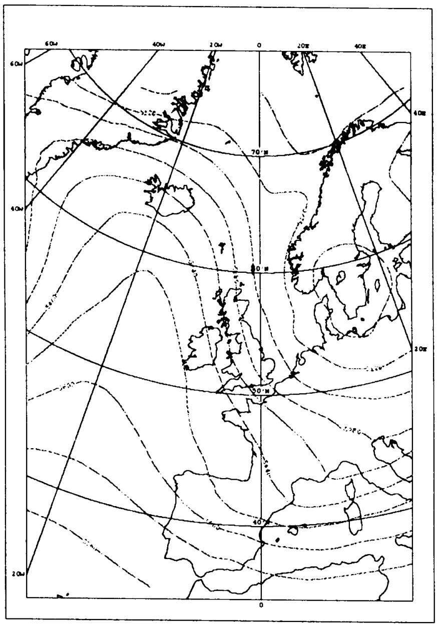

Figure 6: Forecasted Geopotential height of 500 hPa valid at 1800 UTC 1 January 1995

analysed trajectories which arrive in Eelde and Beek are plotted. The trajectories are presented with a solid line when they stay on the same level or move downward. When the motion is upward the trajectories are plotted with a dotted line. Every three hours a cross marks the position of the air parcel along the trajectory. The analysed Eelde trajectory shows a circular path and starts from the Baltic nearby the Swedish coast. The forecasted Eelde trajectory begins at a more northerly position in Sweden. At -36 hours the horizontal and vertical deviations are 687 km and 14 hPa, respectively. During the transport the analysed and forecasted trajectories of Eelde do not follow the same path. At -24 hours the vertical deviation increases to 209 hPa while the horizontal deviation slightly reduces to 637 km. It is ob-

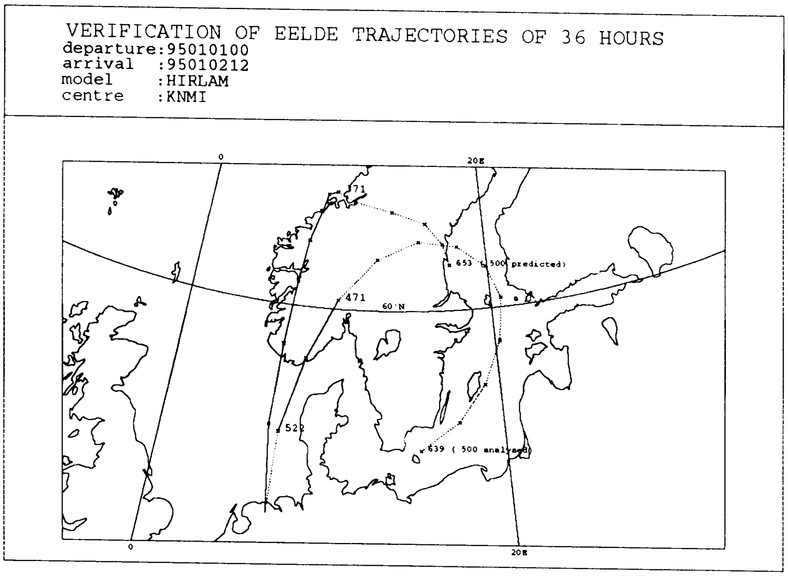

Figure 7: forecasted and analysed 500 hPa trajectories of 36 hours arriving at 2 January 1200 UTC in Eelde

vious that the vertical motion is quite different. The forecasted trajectory crosses a mountain ridge and goes much more upward than the analysed trajectory. The forecasted trajectory has a sharp bent near the Norwegian Atlantic coast. The windfield might be influenced by gravity waves generated by the mountain ridge. Approaching the arrival position the deviations decreases, which is expected.

The Beek trajectories show a completely different pattern Fig. 8. The analysed trajectory begins above Sweden, but the forecasted trajectory originates from the east coast of Greenland, resulting in a horizontal deviation of 2750 km. time and position.

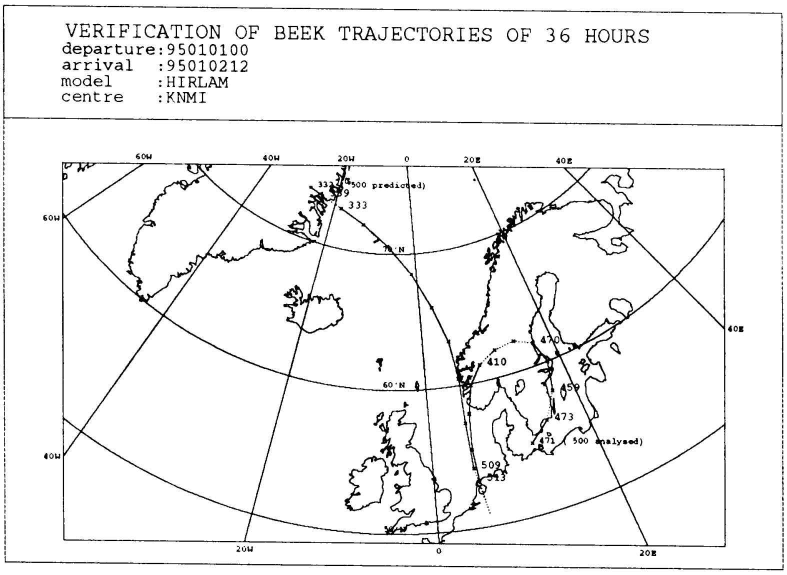

Figure 8: forecasted and analysed 500 hPa trajectories of 36 hours arriving at 2 January 1200 UTC in Beek

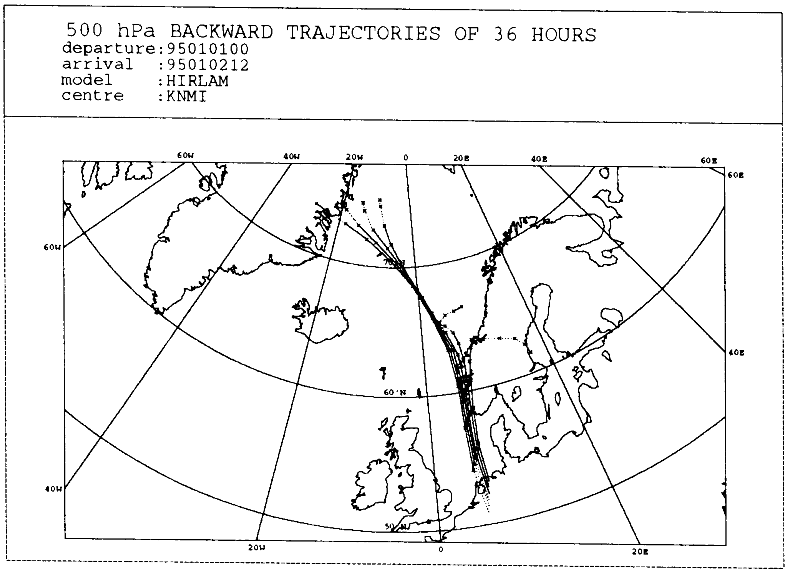

Figure 9: 500 hPa trajectories arriving between Eelde and Beek

At -12 hours the difference between the forecasted and analysed trajectory becomes rather small. The horizontal and vertical deviations are respectively 37 km and 9 hPa at -9 hours. It is clear that the deviations vary enormously with time and position.

To study the uncertainty of the trajectories in more detail 5 trajectories which end on positions evenly spaced between Eelde and Beek are computed. From each point backward trajectories with a duration of 36 hours are calculated. The results are found in Fig. 9. Four of the trajectories start west of Greenland and the other three begin in Scandinavia. They follow a narrow path along Greenland and the northern Atlantic Ocean. The verification results of the Eelde trajectory is better than the Beek trajectory. The pattern of the intermediate trajectories has a divergent character. Four trajectories are coming from the northern Atlantic Ocean, while the others originate from different positions in Sweden. It is clear that extra trajectories reveal a measure of uncertainty.

5 Conclusions

The objective of this project was to calculate and verify HIRLAM trajectories. Backward trajectories were calculated during January and July 1995 which were representative for a wide range of synoptic situations. The meteorological data necessary for the trajectories were obtained from HIRLAM. Trajectories based upon analysed fields are regarded as the 'truth'. Trajectories based upon predicted fields could be compared with the true trajectories.

The average horizontal transport deviation (AHTD) for 36 hour trajectories is about 600 km and 300 km for January and July, respectively. The average vertical transport deviation (AVTD) are about 100 hPa and 50 hPa for January and July, respectively. The relative horizontal and vertical deviations are respectively 4 and 10 percent for January. They slightly decrease in July. It should be noted that the standard deviation in time is in the order of magnitude of the average deviations. This means that the deviations will strongly vary between different forecast series. The variability of the trajectories is shown by an extreme case on 1 January 1995. Trajectories gain more accuracy when a shorter timespan or a lower level is taken. A 12 hours trajectory on 975 hPa has a AHTD and AVTD of 37 km and 6 hPa, respectively. The relative horizontal and vertical deviations are about 2 and 6 percent, respectively. The standard deviations in time of these quantities is in the same order of magnitude as the average deviations.

It is recommended to use relative short trajectories for the transformation of airmasses and for the advection of satellite clouds in operational practice. The HIRLAM trajectories will soon be available for the weather service. It should be noted that the update cycle of the HIRLAM is 6 hours, so trajectories can be made available four times a day.

6 Acknowlegdements

Paula Bailly is thanked for purchasing the redesigned FORTRAN source code of the trajectory model. Seijo Kruizinga's support during this research is appreciated by the author. Erik van Meijgaard is acknowledged for his useful comments on the draft of this report. Ben Wichers Schreur is gratefully thanked for a critical reading of the manuscript.

References

[1] Kruizinga, S. (1991) ECMWF trajectoriën programma basisformules, memorandum KNMI: DM-91-02 (unpublished)

[2] Pettersen, S. (1956) *Weather Analysis and Forecasting*. Vol. I Motion and motion sysems. McGraw-Hill, 428 pp

[3] Rolph, G.D. and R.R. Draxler (1990) Sensitivity of three-dimensional trajectories to the spatial and temporal densities of the windfield. *J. Appl. Meteor.*, 29, 1043-1054

[4] Kallberg, P. (1989) The HIRLAM level1 system documentation manual. Available from SMHI, S-60176, Norrköping, Sweden, March 1990

A a/b coefficients hybrid coordinate system

i	a(i)	b(i)
1	2499.9929199219	0.0000000000
2	7445.2578125000	0.0008603930
3	12028.4140625000	0.0074591935
4	15756.1875000000	0.0277073681
5	18233.6093750000	0.0679893494
6	19246.1914062500	0.1316664815
7	18767.8554687500	0.2187935114
8	16953.3281250000	0.3261452913
9	14115.1171875000	0.4475528598
10	10684.9375000000	0.5745494962
11	7159.6835937500	0.6973265409
12	4031.8991699219	0.8059986830
13	1704.7770996094	0.8921793699
14	391.6481933594	0.9508657455
15	0.0000000000	0.9826333523
16	0.0000000000	0.9961407185

Table 3: Coefficients of the hybrid coordinate system of the HIRLAM